A Dual-Beam Micro-CPW Leaky-Mode Antenna

Ching-Chyuan Lin and Ching-Kuang Cliver Tzuang, *Fellow, IEEE*

***Abstract*—Quasi-planar leaky-mode antenna employing *the second higher order leaky mode* of even symmetry in its leaky-wave regime has been proposed for a new antenna configuration consisting of a microstrip and a coplanar waveguide (CPW) on both sides of the substrate. The new antenna, also known as the micro-CPW antenna, is directly fed by a CPW line without matching circuit. One particular K-band antenna of 36 mm long [about 2.7 free-space wavelengths (λ_0) at 22.1 GHz] shows 5.3% impedance bandwidth for VSWR's less than 2.0 for frequencies between 21.927–23.110 GHz, 11.0-dB antenna gain, and 90.02% efficiency. Detailed analyses show that the dual-beam antenna is linearly polarized along two slanted lines, which lie in the longer axes of the ellipses that approximate the radiation contours. Both theoretical and experimental data for the micro-CPW antenna agree very well for the particular design. The proposed micro-CPW antenna is suitable for active integrated antenna integration at higher microwave and millimeter-wave frequencies.**

***Index Terms*—Coplanar waveguide, leaky-wave antennas, printed antennas.**

I. Introduction

UNIFORM waveguides acting as the leaky-wave antennas have been known to exist in at least three forms: 1) nonradiative-dielectric (NRD)-guide antennas [1]; 2) groove-guide antennas [1]; and 3) printed-circuit antennas [1]. Applications of the leaky modes propagating on these waveguides as antenna designs have gained great success recently. Yoneyama *et al.* [2], for example, pioneered the use of perturbed NRD guide as a very efficient leaky source for feeding a variety of microwave and millimeter-wave planar antennas. On the other hand, Itoh *et al.* [3] had reported a W-band (75–110 GHz) frequency-scanning leaky-wave printed-circuit antenna for vision system; Menzel and Oliner *et al.* [4] demonstrated both experimentally and theoretically that the leaky-wave antenna based on the *first higher order odd leaky mode* on the printed microstrip could be a good line source, being very efficient and showing very little power losses to the surface waves.

The generation of *higher modes* on the microstrip can take many forms. The well-known micro–slot (microstrip-slotline) configuration can effectively emit multiple *higher order leaky modes* of odd symmetry, including the *first higher order leaky mode* by feeding the slotline, as reported in [5, fig. 1]. Exciting the odd modes stems from the fact that a PEC (perfect electric conductor) wall can be placed at the center of the guide during the field theory analyses of the guiding structure. Detailed analyses and potential application of the micro–slot antenna to active integrated antennas had been reported in [5]–[7]. Here, by extending the concept of symmetry and replacing the slotline by a coplanar waveguide (CPW), we propose in Fig. 1 a new generic micro-CPW (*micro*strip-*CPW*) antenna, which, in the later sections of the paper, will demonstrate its effectiveness in emitting the *higher order leaky modes* of even symmetry, including the *second higher order leaky mode* using the CPW as the input feed line. The CPW is connected to the exciting or the receiving port. Since the electromagnetic field of the CPW mode possesses the even symmetry, the complete micro-CPW structure can have a perfect magnetic conductor (PMC) wall placed at the center of the guide. Notice that the CPW can easily interface itself to most discrete transistors and monolithic microwave integrated circuits (MMIC's) since the signal port and grounds are on the same surface. Early development in the micro-CPW antenna technology had demonstrated very good performance at 34 GHz [8]. Although the use of the second higher order leaky mode had shown insensitive to the photolithographic tolerance when developing this millimeter-wave antenna, the operational principle and the characteristics of the micro-CPW antenna are far more complicated than the micro–slot antenna.

Section II presents the numerical data for the dispersion characteristics of the micro-CPW antenna. These data provide the physical insight for understanding how the micro-CPW leaky-mode antenna works and how its antenna beams behave. In Section III, by employing the three-dimensional (3-D) full-wave integral equation analyses and conducting the near-field measurements, we report the detailed antenna characteristics of the input return loss, the radiation patterns, the slanted linear polarization, and both gain and efficiency for a typical micro-CPW antenna operated between 22.1–22.45 GHz, showing very good agreement between theoretical predictions and measured data. Section IV concludes the paper.

II. Design of the Micro-CPW Leaky-Mode Antenna

A. Principle of Operation

As shown in Fig. 1, a microstrip and a CPW coalesce together and form the micro-CPW antenna, which may act as a line source or the unit cell of a linear array. The feed is made by the CPW, which, in practice, is directly connected to a coaxial connector without a matching circuit or is a part of the uniplanar microwave integrated circuit. The microstrip, on the other hand, can radiate the second higher order leaky mode excited by the CPW input. Consequently, the micro-CPW can integrate the active components such as amplifiers and switches easily on the same surface where the CPW's reside. No dc blocking is required when integrating the micro-CPW with the active devices since the CPW underneath the microstrip is open circuited at the far end (see Fig. 1).

The normal CPW mode is of even symmetry. Hence, we may insert a magnetic wall along the x–z plane in Fig. 1 to simplify the full-wave analyses of the resultant half-circuit composed of

Manuscript received August 5, 1997; revised December 1, 1998.

The authors are with the Institute of Electrical Communication Engineering, National Chiao Tung University, Hsinchu, Taiwan, R.O.C.

Publisher Item Identifier S 0018-926X(00)02621-1.

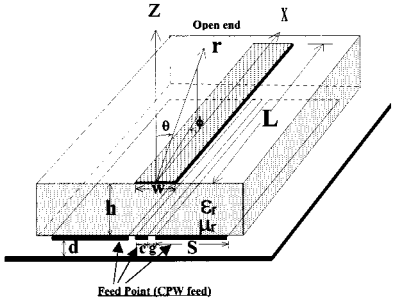

Fig. 1. The generic micro-CPW leaky-mode antenna emitting the second, fourth, etc., higher order leaky modes of even symmetry with a conductor-backed plane that may not be present. θ: the elevation angle measured from broadside; ϕ: the azimuthal angle referenced to the symmetric plane of the magnetic wall in the x–z plane.

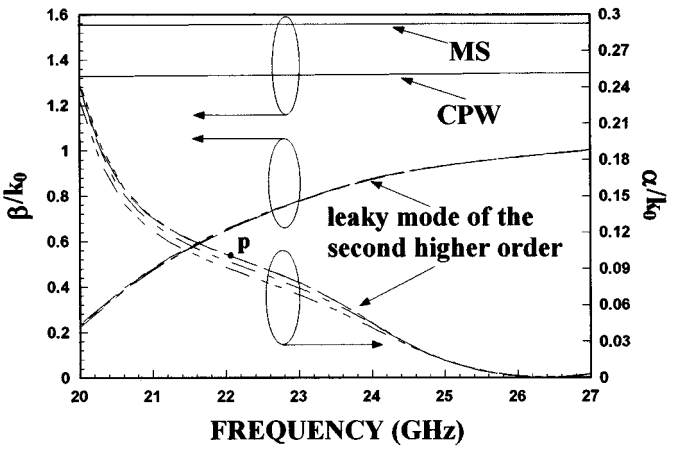

Fig. 2. The normalized phase and attenuation constants of the even-symmetric micro-CPW antenna, showing the second higher order leaky mode and two well-known bound modes, the MS mode and the CPW mode. $\varepsilon_r = 2.55$, $h = 0.762$ mm, $c = 0.508$ mm, $g = 0.508$ mm, $s = \infty$, $w = 9$ mm, metal thickness = 0.03 mm, conductivity = 5.8×10^7 S/m (copper), and the top cover height = $9h$. $d = 5.0000$ mm: - - - $d = 2.7432$ mm: $\cdots$ $d = 1.3716$ mm: -·-·- $d = 0.6858$ mm: -·····-.

three-plus-one conductors. In the case of the even-symmetric excitation, the micro-CPW supports the microstrip (MS) mode with its electromagnetic energy concentrating between the microstrip and the CPW, the CPW mode with its electromagnetic fields crowded between the two gaps, and the higher order leaky modes of the microstrip. This manifests an overmoded device of which we intend to excite the leaky modes. It is the second higher order leaky mode we wish to excite since such mode becomes leaky in a frequency band just before the cutoff. Given a dielectric sheet of relative permittivity ε_r, the structural parameters w (width of microstrip), h (substrate height), c (center conductor width of CPW), g (gap width of CPW), and s (side plane width of CPW) must be carefully chosen such that the desired even higher order leaky mode can be properly excited by electromagnetically coupling the CPW feed line to the microstrip, thus forming a leaky-mode antenna.

B. The Dispersion Characteristics

The best way to understand the operational principle of the micro-CPW antenna should begin with the dispersion characteristics of the antenna, which are obtained by rigorous full-wave mode-matching method employing the metal modes taking into account both finite metal thickness and conductivity. The mode-matching method had been well documented [9] and will not be reported here. When performing the mode-matching analyses, a top cover is placed at a sufficiently far distance such that the cover height has negligible influence on the modal characteristics of the micro-CPW line. In the particular case study presented in this paper, the cover height of nine times the substrate thickness can serve the purpose well.

Fig. 2 shows the modal spectra of the micro-CPW line printed on a 0.762-mm-thick ULTRALAM$^{\mathrm{TM}}$ 2000 (a trademark of Rogers Corporation) substrate with relative permittivity ε_r of 2.55. The metal thickness of 0.03 mm and conductivity of 5.8×10^7 S/m (copper) are also assumed. On the microstrip side, the width of the strip is 9 mm—not wide enough to protrude beyond the CPW's side planes that also serve as the referenced ground for the microstrip mode. On the opposite side lies the coplanar waveguide, of which the central strip width (c), gap (g), and side plane width (s) are chosen to make a 100 Ω CPW line if the microstrip line were not present on the other side. The choice is made that the micro-CPW antenna will be excited by the CPW line extended from the generic micro-CPW. Such arrangement makes the measurement of the micro-CPW antenna fairly easy since a CPW or a coaxial line can be directly launched into the CPW feed line and they are readily accessible in most laboratories. Three types of even modes constitute the first three major modes of the micro-CPW line. The MS mode comes first, which should be viewed as the mode for a microstrip with two tuning septa formed by the gaps of the underneath CPW. The CPW mode, however, distributes its electromagnetic fields concentrated mostly near the gaps with substantial amount of influence by the wide microstrip line viewed as a conductor back plane to the CPW. The second higher order leaky mode of the MS mode with an onset frequency at approximately 27 GHz is the third mode to appear in Fig. 2. The particular design shows a fairly broad spectrum in which the normalized attenuation constant is considered small, i.e., 0.1. Notice that the normalized attenuation constant α/k_0 of a leaky-mode antenna is usually kept below 0.1 to compromise antenna gain and length [10]. The leaky mode's dispersion curves imply that the leaky-mode antenna can be very useful for a wide frequency range if the leaky mode is excited properly.

C. Assessment of the Antenna from the Leaky Mode

The micro-CPW is intended for the use in active integrated antennas where the CPW is connected to the active circuits. Furthermore, the micro-CPW can be located at a distance d above the supporting conductor plane, as shown in Fig. 1. Consequently, the effect of d on the leaky-mode propagation must be examined before the antenna is designed. Fig. 2 plots the normalized complex propagation constants against the variation of distance d from 0.6858–5 mm, respectively, showing virtually negligible effect. Further studies indicate that when d is increased significantly, the complex propagation constants appear very close to that shown in Fig. 2. Thus, the complex dispersion characteristics with d of 5 mm in Fig. 2 can be used for the micro-CPW antenna design with good accuracy.

The fan-shaped antenna radiation patterns have been well known for the leaky-wave antennas based on the leaky-mode

design [5], [7], [10]–[12]. For example, the point p of Fig. 2 will correspond to the fan beam(s) peaked at the elevation angle (measured from the broadside) of

$$\theta_m \cong \sin^{-1}(\beta/k_0) \tag{1}$$

i.e., 42.2° in this case at 22 GHz, where $\beta/k_0 = 0.672$ and $\alpha/k_0 = 0.1$. It is therefore clear that the complex phase and attenuation constants provide most useful information for characterizing the leaky-mode antenna. As frequency is increased from 22 to 26.94 GHz, which corresponds to the cutoff frequency of the leaky mode, the main beam(s) will scan from $\theta_m = 42.2°$ to $\theta_m = 90°$ (horizon). On the other hand, the attenuation (leakage) constant directly leads to a quick estimation of the desired antenna length. It has been shown that if L (the length of leaky-wave antenna) is chosen as

$$L \cong 0.183\,\frac{\lambda_0}{\alpha/k_0} \tag{2}$$

90% of the electromagnetic energy will leak, leaving 10% energy either absorbed at the far end or reflected backward [13]. At 22 GHz, application of (2) leads to a conclusion that the antenna should be at least 25 mm long (or 1.83 λ_0) if no more than 10% of energy is wasted for the micro-CPW antenna. One notes that the characteristics of the micro-CPW leaky-mode antenna employing the second higher order leaky mode are far more complicated than the above discussions. The longitudinal current distributions of the first higher order leaky mode on the microstrip line of the micro–slot antenna change longitudinally signs once but the transverse distribution does not change [14], [15], resulting in the micro–slot antenna that radiates an on-axis single-fan beam radiation pattern, as shown in [5], [7], [10]–[12]. However, the fact that the longitudinal and transverse current distributions of the second higher order leaky mode on the microstrip line of the micro-CPW antenna, respectively, change longitudinally signs twice and change transversely signs once [14], [15] implies that an off-axis dual-fan beam radiation pattern may exist. If this does happen, the radiation pattern and polarization of the micro-CPW are no longer a simple matter that can be directly derived from the complex dispersion characteristics.

III. Characteristics of the Micro-CPW Antenna

A comprehensive treatment on the investigation of the micro-CPW antenna characteristics is given in this section, including the input return loss, radiation patterns, polarization, gain and efficiency. Rigorous full-wave space-domain integral equation method is invoked to validate the measured results and vice versa. Before initiating the full-wave analyses, the accurate CPW modal currents in both longitudinal and transverse directions should be obtained for extracting the scattering parameters. Detailed discussions about the particular CPW S-parameter extraction using the integral equation method had been reported elsewhere [16].

A. Antenna Input Return Loss

As revealed in Figs. 1 and 2, the micro-CPW structure may support the MS, CPW, and leaky modes. Therefore, the micro-CPW manifests itself as an overmoded device in which the mode conversion of the input CPW mode to the leaky mode is of the most desired. However, the matrix-pencil signal analyses [17]–[19] of the excited currents obtained by the full-wave space-domain integral equation method in the micro-CPW structure indicate that both CPW mode and leaky mode prevail, whereas the amount of MS mode is too little to be detected. The results of the matrix-pencil analyses also yield the complex propagation constant for the leaky mode as well as the real propagation constant for the CPW mode. The micro-CPW antenna presented here does not include any termination. Except for the input CPW feed, the rest of the micro-CPW ports are open-circuited. The overall effect of generating multiple modes and mode conversions involving the leaky mode generally makes the useful bandwidth of the micro-CPW antenna narrower. Since the excited CPW mode with the normalized phase constant $\beta_{\rm CPW}/k_0$ of 1.331 propagates back and forth in the micro-CPW structure and causes the resonant effect, the bandwidth is reduced. The resonant frequencies of the CPW mode are dictated by the resonant condition $\beta_{\rm CPW} l = n\pi$, where $\beta_{\rm CPW}$ is the phase constant of the CPW mode and l is the length of the guiding structure. The predicted CPW resonant frequencies are, therefore, 21.92 GHz ($n = 7$) and 25.05 GHz ($n = 8$), respectively, which are close to the measured frequencies at 22.44 and 25.27 GHz, as shown in Fig. 3, where the useful bandwidth of the micro-CPW is apparently narrower than what the leaky mode alone should have. Notice that the theoretical full-wave space-domain integral equation method show that the resonant frequencies are located at 22.46 and 25.57 GHz, respectively. Also notice that l is 36 mm long, much greater than the length of 25 mm as discussed in the previous Section II-C for improved radiation. The particular design demonstrates very good input return loss of below −10 dB for frequencies between 21.927–23.110 GHz as well as between 24.998–25.988 GHz, encompassing the two resonant regions caused by the CPW mode mentioned above. Fig. 3 also illustrates very good agreement for both measured and theoretical data, although the theoretical results show somewhat narrower bandwidths for regions with good matching. Since the total antenna efficiency needs to consider the input mismatch losses, the excellent input matching demonstrated here may help design a highly efficient leaky-mode antenna.

B. Radiation Patterns with and Without Conductor Backing

As implied in Section II-C, discussing the reversal polarities of higher order leaky-modal currents, the radiation patterns of the micro-CPW antenna appear complicated as compared to the micro-slot antenna [5], [7], [10]–[12], which exhibits a well-defined fan beam. Fig. 4 plots the far-field radiation contour of the micro-CPW antenna at 22.1 GHz obtained by using the 3-D full-wave integral equation method [20]. Notice that the conductor-backed plane is removed ($d = \infty$). Fig. 4 clearly shows that the micro-CPW employing the second higher order leaky mode is a dual-beam antenna, pointing its two symmetric main beams (θ_m, ϕ_m) (m represents the maximum peak of total E field) to (49.1°, 45°) and (49.1°, −45°), respectively. The two additional leakages of −8.0 dB down the normalized main beam

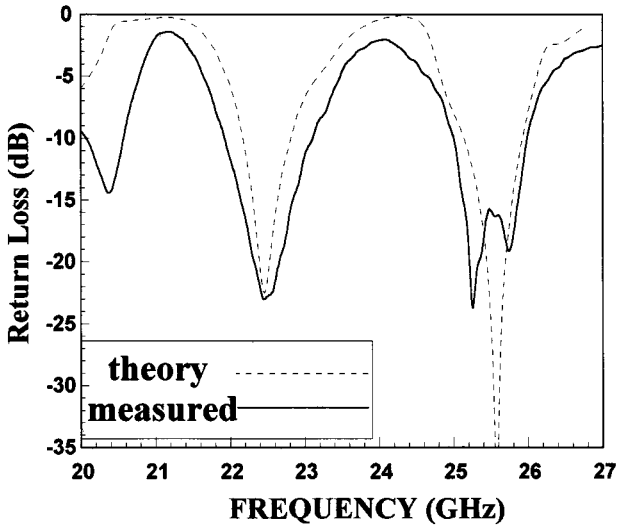

Fig. 3. The measured and theoretical input return loss data of the micro-CPW antenna shown in Fig. 1. $\varepsilon_r = 2.55$, $h = 0.762$ mm, $c = g = 0.508$ mm, $s = 7.325$ mm, $w = 9$ mm, $L = 36$ mm. No conductor backing is present.

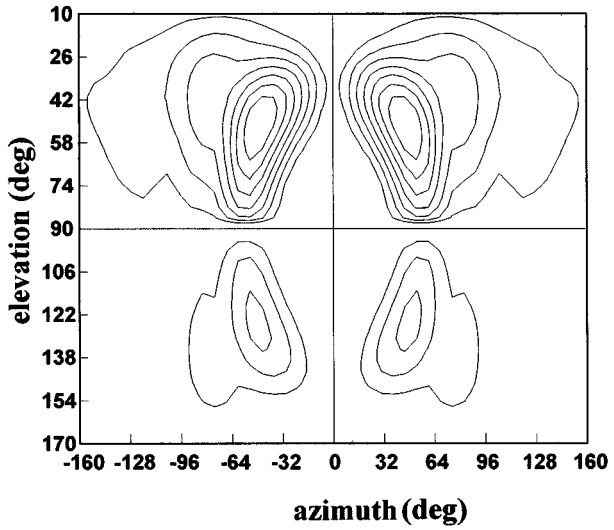

Fig. 4. The theoretical radiation contour of the micro-CPW antenna with the conductor-backed plane removed ($d = \infty$). $f = 22.1$ GHz.

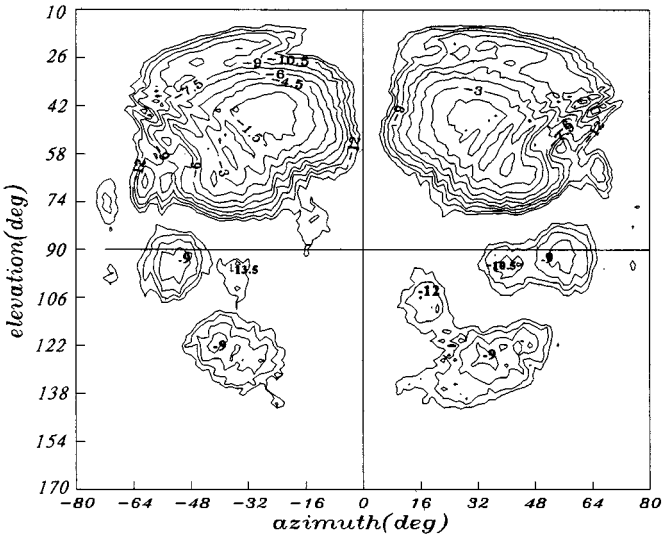

Fig. 5. The measured micro-CPW radiation contour in the y–z plane facing the open end of the antenna without the conductor-backed plane. $f = 22.1$ GHz.

are observed at (126.8°, 45°) and (126.8°, −45°), respectively. These residual leakages are clearly contributed by the CPW line and its feed. Additional two back lobes are observed, pointing to (49.1°, 135°) and (49.1°, −135°), respectively. Notice that the predicted main beam using the modal data has θ_m [by (1)] of 42.5°, slightly lower than that predicted by the 3-D field theory. The discrepancy may be attributed to the approximate expression: $\theta_m \cong \sin^{-1}(\beta/k_0)$, which is very good for narrow beams, but not as accurate for the case of wider beams [21] in our design. The far-field radiation patterns extracted out of the near-field antenna measurement system [Nearfield Systems, Inc.] are plotted in Fig. 5 for the same micro-CPW antenna analyzed earlier. Two main beams and two residual leakages are observed. The latter are −9.0 dB down as referenced to the main beam, showing good agreement with the theoretical prediction. The main beams point to (θ_m, ϕ_m) of (48.4°, −39.8°) and (48.4°, 38.2°), respectively. Comparing these measured angles with the theoretical values, the elevation angle θ_m agrees excellently, only 0.7° lower, whereas the azimuthal angle ϕ_m shows approximately 6.8° difference. It is likely that the limited scan plane in the azimuthal direction of our near-field system made the truncated error of the end effect [22], causing the discrepancy for the azimuthal angles. Nevertheless, the overall measured antenna radiation patterns are in good agreement with the theoretical computations. As the operating frequency is increased from 22.1 to 22.45 GHz by 350 MHz, one observes the beam scanning characteristics of the leaky-mode antenna with the measured main beam traversing from θ_m of 48.4–52°.

By placing a conducting plane at distance d equal to 5 mm away from the micro-CPW antenna, the amplitudes of the two residual beams are reduced to −20 dB as depicted in Fig. 6. A great reduction of 11 dB on residual leakage is achieved. Moreover, the measured main beams as shown in Figs. 5 and 6 are at the same θ_m of 48.4°, which coincide the result as predicted in Fig. 2, where the normalized phase constant (β/k_0) and attenuation constant (α/k_0) are very close to 0.6756 and 0.0996 for distance $d \geq 2.7432$ mm at 22.1 GHz. Therefore, the effect of distance d on radiation pattern is negligible for the particular structure. Although the improvement over the residual leakages is improved, both measurements as depicted in Figs. 5 and 6 showed end-fire radiations of comparable magnitudes, approximately −9 dB down from the peak values. Nevertheless, such end-fire radiations are still subject to extensive studies as the actual causes are still unknown to authors.

C. Polarization

Figs. 4–6 reveal two fan-shaped beams in the θ–ϕ radiation contour plane. Question about whether these two fan beams are linearly polarized needs confirmation since so far there is no direct evidence to say so. Since the main beams (theoretical data) are located at $\theta_m = 49.1°$ plane at 22.1 GHz, we plot the theoretical values of E_θ and E_ϕ components against the azimuthal angle ϕ at $\theta_m = 49.1°$ plane. The results are plotted in Fig. 7(a) and (b) for the phase and magnitude components, respectively.

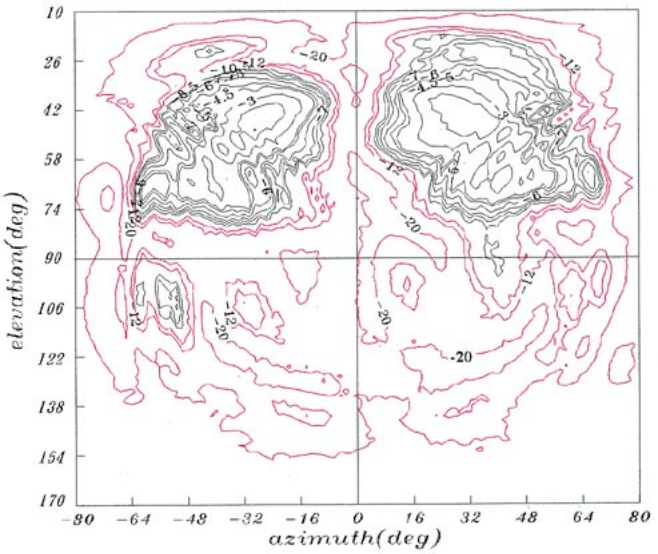

Fig. 6. The measured micro-CPW radiation contour in the y–z plane facing the open end of the antenna backed by a conducting plane at $d = 5$ mm. $f = 22.1$ GHz.

Observing Fig. 7(a) closely, there are in-phase regions for $\phi \in [29°, 63°]$ and out-of-phase region for $\phi \in [-63°, -29°]$. Notice that the theoretical value of ϕ_m ($\pm 45°$ at 22.1 GHz) is in the middle of the in-phase and out-of-phase regions as indicated in Fig. 7(a) and (b). The ratio of the magnitude of $E_{\theta m}$ over $E_{\phi m}$ is 1.2239 as observed from Fig. 7(b) for both in-phase and out-of-phase regions, where $E_{\theta m}$ and $E_{\phi m}$ are the vectored electric (E) field at $\theta_m = 49.1°$ and $\phi_m = \pm 45°$. In the θ–ϕ radiation contour plane, the electric vector can be, respectively, decomposed into two orthogonal components along θ and ϕ directions as follows [23]:

$$E_\theta = E_{\theta 0} \cos(\omega t + k_0 z + \psi_\theta) \tag{3}$$

and

$$E_\phi = E_{\phi 0} \cos(\omega t + k_0 z + \psi_\phi) \tag{4}$$

where k_0 denotes the free-space wavenumber. $E_{\theta 0}$ and $E_{\phi 0}$ are, respectively, the maximum magnitudes of the θ and ϕ components. ψ_θ and ψ_ϕ are the phase components. If $\psi_\theta - \psi_\phi = n\pi$, where $n = 0, 1, 2, 3$, etc., the polarization of the vector E field must be linear. Notice that the vector E fields are in-phase if $\psi_\theta - \psi_\phi = 2n\pi$, out-of-phase if $\psi_\theta - \psi_\phi = (2n+1)\pi$. Hence, one may expect that the slanted linear polarization in the θ–ϕ radiation contour plane is associated with the micro-CPW antenna. If the phase angles are either in-phase or out-of-phase, the polarization vector should pass (θ_m, ϕ_m) at an angle δ given by

$$\delta = \tan^{-1} \frac{E_\theta}{E_\phi}. \tag{5}$$

The value of δ is readily available from Fig. 7(b), where δ equals to $\tan^{-1}(E_{\theta m}/E_{\phi m})$ or 50.7° at positions $\theta_m = 49.1°$ and $\phi_m = \pm 45°$. Knowing the values of ϕ_m and δ, we proceed the copolarization and cross-polarization measurements, assuming for the moment that the main beams are linearly polarized. First we rotate the micro-CPW antenna in the azimuthal plane by ϕ_m, resulting in a main beam pointing into the $\phi = 0°$ in the observer's θ–ϕ plane. Then we rotate the near-field probe by δ degrees [using (5)] and measure the radiation pattern as the copolarization. Followed by rotating the near-field probe by another 90°, the cross-polarization pattern is obtained. The results are shown in Fig. 8, indicating that the cross-polarization profile is -16.5 dB below the peak radiation power throughout the 10–170° elevation angles. The results confirmed that there indeed exists a slanted linearly polarized fan beam. The same procedure can be applied for the second fan beam.

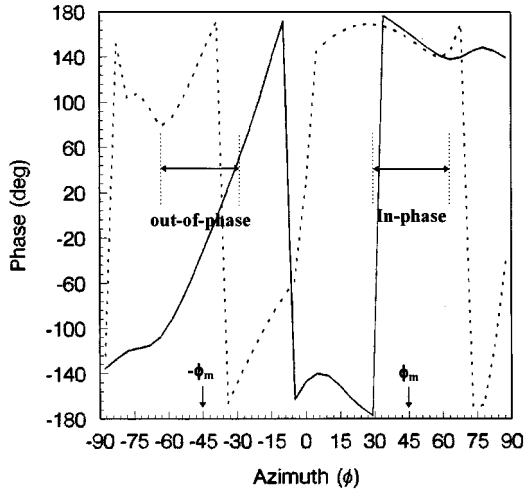

(a)

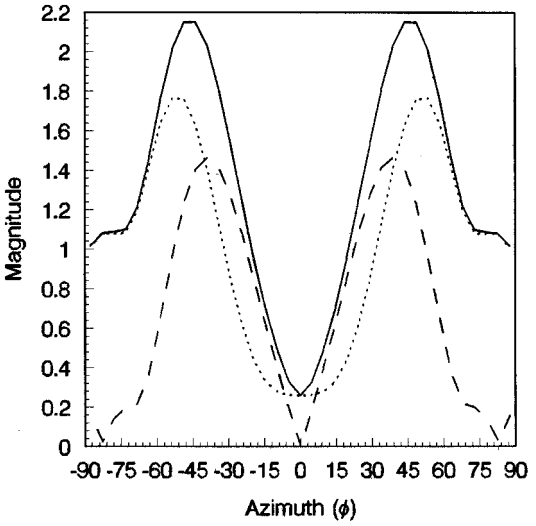

(b)

Fig. 7. (a) The phase variation of E_θ (solid line) and E_ϕ (dotted line) against the azimuthal angle ϕ at $\theta_m = 49.1°$ for the micro-CPW antenna operating at $f = 22.1$ GHz with the conductor-backed plane removed ($d = \infty$). The out-of-phase and in-phase regions are, respectively, between -63 to $-29°$ and between 29–63°, where $\phi_m = \pm 45°$. (b) The magnitude variation of E_{total}(solid), E_θ (dotted), and E_ϕ (broken) against the azimuthal angle ϕ at $\theta_m = 49.1°$ for the micro-CPW antenna operating at $f = 22.1$ GHz with the conductor-backed plane removed ($d = \infty$). The maximum E_{total} lies at $\phi_m = \pm 45°$.

Redrawing the radiation contour of Fig. 4 and plotting two lines using (5) in the in-phase and out-of-phase regions [referring to Fig. 7(a)], Fig. 9 interestingly shows that the two fan beams are linearly polarized along two slanted lines which lie in the longer axes of the ellipses that approximate the radiation contours.

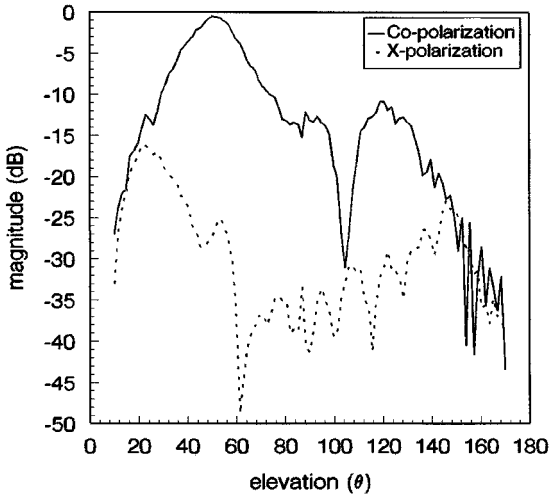

Fig. 8. The copolarization and cross-polarization measurements of one of the dual beams for the micro-CPW antenna with the conductor-backed plane removed ($d = \infty$). The antenna is rotated by $\phi_m = 45°$, using a test fixture at $f = 22.1$ GHz. Then the near-field probe is rotated by $\delta = 50.7°$. The peak lies at $\theta_m \cong 49.1°$.

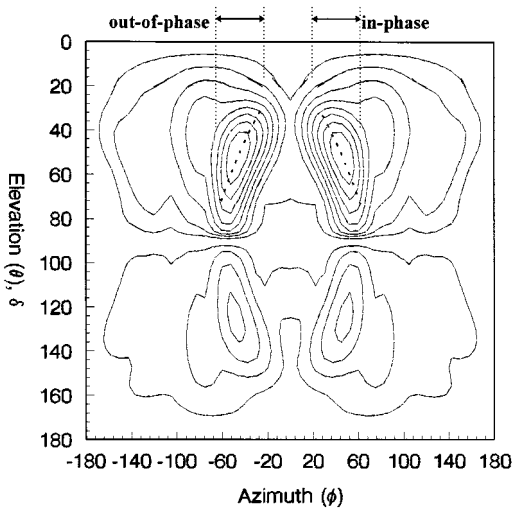

Fig. 9. Two linearly polarized fan beams are along the dotted slanted lines [obtained by (5)] in the longer axes of the ellipses approximating the shapes of the radiation contours of the micro-CPW antenna.

D. Gain and Efficiency

To determine the gain of the micro-CPW, we apply the gain-transfer measurement or the so-called antenna gain-comparison method [23] in which the gain of the micro-CPW antenna is determined by comparing it to the gain of a known standard antenna. Accordingly, the measured antenna gains at 22.1 and 22.45 GHz are 11.0 and 10.84 dB, respectively. The corresponding theoretical results obtained by the full-wave integral equation method are 10.11 and 9.97 dB. The measured antenna efficiencies at 22.1 and 22.45 GHz are, respectively, 90.02 and 87.92%. The corresponding theoretical results obtained by the full-wave integral equation method are 93.20 and 91.43%. The results show that the agreement between the theoretical and experimental data is good. Notice that the measured antenna efficiencies have included the energy of the back lobes pointing to (49.1°, 135°) and (49.1°, −135°) where the planar scan surface cannot detect by the near-field probe since it can only receive the front hemispheric energy emitted from the micro-CPW antenna. The energy of the back lobes at 22.1 GHz (22.45 GHz) is approximately 3.62% (4.47%) to the main lobe's energy, estimated by invoking the lossy transmission line equation $e^{-2\alpha L}$. Notice that the conductor losses are not included in the theoretical full-wave analyses.

IV. Conclusions

A dual-beam micro-CPW leaky-mode antenna employing the second higher order leaky mode of even symmetry is presented. Although the inherent multimodes micro-CPW antenna limits the useful bandwidth of the micro-CPW antenna, the antenna can be designed with proper terminations to achieve excellent input return losses at different frequencies. In the particular design presented here the terminations are open loads, further simplifying the antenna design. The effect of the distance d between the conductor-backed plane and antenna on the main beams is negligible when d is greater than 5 mm for the particular design. The dual-beam characteristics of the antenna are linearly polarized along two slanted lines which lie in the longer axes of the ellipses that approximate the radiation contours as shown in Fig. 9. The particular 36 mm long micro-CPW antenna shows the gain of 11.0 dB and the efficiency of 90.02% at 22.1 GHz, 0.89 dB higher and 3.18% lower than the theoretical predictions. The input return loss can be maintained less than -10 dB for operating frequencies between 21.927–23.110 GHz as well as between 24.998–25.988 GHz, rendering a high-efficiency antenna of moderate bandwidth. In view of the direct CPW feed for the micro-CPW leaky-mode antenna, the antenna itself can be easily integrated into the uniplanar type integrated circuits. The philosophy behind the design of the micro-CPW antenna is another manifestation of the fact that the leaky-mode antennas are best viewed as waveguides [24]. A dual-beam antenna finds many applications such as automotive doppler radar sensor [25], angle-diversity performances [26], [27], enhancement of the synthetic aperture radar (SAR) system capabilities [28], tracking two satellites for telecommunication network system [29], and microwave closed-range sensors [30].

References

[1] A. A. Oliner, "Scannable millimeter wave arrays," Weber Res. Inst., Polytechnic Univ., New York, NY, Tech. Rep. Poly-WRI-1543-88, vol. I/II, Sept. 1988.

[2] K. Maamria, T. Wagatsuma, and T. Yoneyama, "Leaky NRD guide as a feeder for microwave planar antennas," *IEEE Trans. Antennas Propagat.*, vol. 41, pp. 1680–1686, Dec. 1993.

[3] A. Basu and T. Itoh, "Dielectric waveguide based leaky wave antenna arrays for radiometry at 94 GHz and 212 GHz," in *Proc. Asia-Pacific Microwave Conf.*, New Delhi, India, Dec. 1996, pp. 87–90.

[4] F. K. Schwering and A. A. Oliner, "Millimeter-wave antennas," in *Antenna Handbook*, Y. T. Lo and S. W. Lee, Eds. New York: Van Nostrand Reinhold, 1988, ch. 17.

[5] C. K. C. Tzuang, G. J. Chou, S. P. Liu, and K. F. Fuh, "Active integrated leaky-mode antenna," in *Proc. Int. Symp. Antennas Propagat.*, Chiba, Japan, Sept. 1996, pp. 1237–1240.

[6] C. K. C. Tzuang, S. P. Liu, and G. J. Chou, "Integrated active leaky-wave antenna employing arched microstrip line," in *Proc. Asia-Pacific Microwave Conf.*, Taejon, Korea, Oct. 1995, pp. 335–338.

[7] G. J. Chou and C. K. C. Tzuang, "Oscillator-type active-integrated antenna: The leaky-mode approach," *IEEE Trans. Microwave Theory Tech.*, vol. 44, pp. 2265–2272, Dec. 1996.

[8] C. K. C. Tzuang and C. C. Lin, "Millimeter wave micro-CPW integrated antenna," in *Proc. SPIE Conf.*, Denver, CO, Aug. 1996, pp. 513–518.
[9] C. K. C. Tzuang, C. C. Tien, and K. K. Chan, "Full-wave investigation of leakage from a covered microstrip line with finite strip conductivity and thickness," in *Proc. 20th European Microwave Conf.*, Budapest, Hungary, Sept. 1990, pp. 543–548.
[10] G. J. Chou and C. K. C. Tzuang, "An integrated quasiplanar leaky-wave antenna," *IEEE Trans. Antennas Propagat.*, vol. 44, pp. 1078–1085, Aug. 1996.
[11] K. F. Fuh and C. K. C. Tzuang, "Magnetically scannable microstrip antenna employing a leaky gyromagnetic microstrip line," *Electron. Lett.*, vol. 31, no. 16, pp. 1309–1310, Aug. 1995.
[12] A. A. Oliner and K. S. Lee, "Microstrip leaky wave strip antennas," in *IEEE Int. Antennas Propag. Symp. Dig.*, Philadelphia, PA, June 1986, pp. 443–446.
[13] A. A. Oliner, "Leakage from higher modes on microstrip line with application to antennas," *Radio Sci.*, vol. 22, no. 6, pp. 907–912, Nov. 1987.
[14] K. A. Michalski and D. Zheng, "Rigorous analysis of open microstrip lines of arbitrary cross section in bound and leaky regimes," *IEEE Trans. Microwave Theory Tech.*, vol. 37, pp. 2005–2010, Dec. 1989.
[15] J. S. Bagby, C. H. Lee, D. P. Nyquist, and Y. Yuan, "Identification of propagation regimes on integrated microstrip transmission lines," *IEEE Trans. Microwave Theory Tech.*, vol. 41, pp. 1887–1894, Nov. 1993.
[16] W. T. Lo, C. K. C. Tzuang, S. T. Peng, C. C. Tien, C. C. Chang, and J. W. Huang, "Resonant phenomena in conductor-backed coplanar waveguides (CBCPW's)," *IEEE Trans. Microwave Theory Tech.*, vol. 41, pp. 2099–2108, Dec. 1993.
[17] Y. Hua and T. K. Sarkar, "Matrix pencil method for estimating parameters of exponentially damped/undamped sinusoids in noise," *IEEE Trans. Acoust., Speech, Signal Processing*, vol. 38, pp. 814–824, May 1990.
[18] ——, "Generalized pencil-of-function method for extracting poles of an EM system from its transient response," *IEEE Trans. Antennas Propagat.*, vol. 37, pp. 229–234, Feb. 1989.
[19] T. K. Sarkar, Z. A. Maricevic, and M. Salazar-Palma, "Characterization of power loss from discontinuities in guided structure," in *IEEE MTT-S Int. Microwave Symp. Dig.*, Denver, CO, June 1997, pp. 613–616.
[20] W. T. Lo, C. K. C. Tzuang, S. T. Peng, and C. H. Lin, "Full-wave and experimental investigations of resonant and leaky phenomena of microstrip step discontinuity problems with and without top cover," in *IEEE MTT-S Int. Microwave Symp. Dig.*, San Diego, CA, May 1994, pp. 473–476.
[21] K. S. Lee, "Microstrip line leaky wave antenna," Ph.D. dissertation Section III, Polytechnic Univ., Brooklyn, NY, June 1986.
[22] D. Slater, *Near-Field Antenna Measurements*. Norwood, MA: Artech House, 1991.
[23] C. A. Balanis, *Antenna Theory Analysis and Design*. New York: Wiley, 1997.
[24] A. A. Oliner, "Historical perspectives on microwave field theory," *IEEE Trans. Microwave Theory Tech.*, vol. MTT-32, pp. 1022–1045, Sept. 1984.
[25] J. P. Daniel, M. Himdi, and D. Thouroude, "Design of multibeam antennas arrays. examples," in *Proc. ISAP Conf.*, vol. 1, Chiba, Japan, Sept. 24–27, 1996, pp. 169–172.
[26] D. Di. Zenobio, E. Russo, and S. Candeo, "Angle diversity performances on a line-of-sight microwave path using a dual-beam dish antenna," in *Inst. Elect. Eng. 7th Int. Conf. Antennas Propagat.*, vol. 2, York, U.K., Apr. 1991, pp. 306–309.
[27] D. Di. Zenobio, G. Santella, S. Candeo, and D. Mandich, "Angle and space diversity: Experimental comparison," in *IEEE Global Telecommun. Conf.*, vol. 3, Orlando, FL, Dec. 1992, pp. 1851–1857.
[28] M. Bonnedal, I. Karlsson, and K. V. Klooster, "A dual beam slotted waveguide array antenna for SAR applications," in *Inst. Elect. Eng. 7th Int. Conf. Antennas Propagat.*, vol. 2, York, U.K., Apr. 1991, pp. 559–562.
[29] T. Hori, H. Higa, and K. Kagoshima, "Design of offset double torus dual-beam antenna by minimizing aperture mapping distortion," in *Inst. Elect. Eng. 8th Int. Conf. Antennas Propagat.*, vol. 2, Edinburgh, U.K., Mar. 30–Apr. 2 1993, pp. 623–626.
[30] B. Zimmermann and W. Wiesbeck, "24 GHz microwave close-range sensors for industrial measurement applications," *Microwave J.*, vol. 39, no. 5, pp. 228–238, May 1996.

Ching-Chyuan Lin was born in Taiwan on November 7, 1958. He received the B.S. degree in physics from the Soochow University, Taipei, Taiwan, in 1982, and the M.S. degree in space science from the National Central University, Chung-Li, Taiwan, in 1984. He is currently working toward the Ph.D. degree in communication engineering at National Chiao Tung University, Hsinchu, Taiwan.

From 1984 to 1994, he was with the Chung Shang Institute of Science and Technology, Lung-Tan, Taiwan. His current research interests include field theory analysis and its application on design of leaky-mode antennas.

Ching-Kuang Cliver Tzuang (S'84–M'86–SM'92–F'99) received the B.S. degree in electronic engineering from National Chiao Tung University, Hsinchu, Taiwan, in 1977, the M.S. degree from the University of California, Los Angeles, in 1980, and the Ph.D. degree in electrical engineering from the University of Texas at Austin, in 1986.

From 1981 to 1984, he was with TRW, Redondo Beach, CA, working on analog and digital monolithic microwave integrated circuits. Since 1986 he has been with the Institute of Communication Engineering, National Chiao Tung University, Hsinchu, Taiwan. His research activities involve the design and development of millimeter-wave and microwave active and passive circuits and the field theory analysis and design of various complex wave guiding structures and large array antennas. To date, 49 master degree students and 13 Ph.D. students have graduated under his supervision.

Dr. Tzuang helped form the IEEE Microwave Theory and Techniques Society, Taipei Chapter. He served as Secretary, Vice Chairman, and Chairman in 1988, 1989, and 1990, respectively. He has been on the Asia-Pacific Microwave Conference International Steering Committee, where he has been the International Liaison Officer representing the Taipei Chapter, since 1994.